

# Effects of nucleation agents on the preparation of transparent glass–ceramics

M. Ghasemzadeh<sup>a,\*</sup>, A. Nemati<sup>b</sup>, S. Baghshahi<sup>c</sup>

<sup>a</sup> Department of Materials Engineering, Karaj Branch, Islamic Azad University, Karaj, Iran

<sup>b</sup> Department of Materials Science & Engineering, Sharif University of Technology, Tehran, Iran

<sup>c</sup> Faculty of Engineering, Imam Khomeini International University, Qazvin, Iran

Available online 26 March 2012

## Abstract

Formation of transparent glass–ceramic in the system  $\text{MgO–SiO}_2\text{–Al}_2\text{O}_3\text{–K}_2\text{O–B}_2\text{O}_3\text{–F}$  with and without addition of LiF and NaF has been investigated. Crystallization of glass-sample was conducted by controlled thermal heat-treatment, at determined nucleation and crystallization temperatures. In this regard, the effects of addition of LiF and NaF were investigated on the crystallization behavior and transparency of the samples.

Low transmission (less than 80% at 600 nm) was observed in the basic composition (K).

The addition of NaF and LiF caused more intense phase separation in the system.

The results indicated that the glass–ceramic can remain transparent if fine grains with nano size are precipitated but will turn into opaque when large grains appear, because of the difference in the refractive index between glass and precipitated crystals.

© 2012 Elsevier Ltd. All rights reserved.

**Keywords:** Microstructure-final; Optical properties; Glass; Glass ceramics

## 1. Introduction

Future applications for glass–ceramics are likely to capitalize on, highly specialized properties for information transmission, display, and storage. Glass–ceramics of uniformly dispersed crystals less than 100 nm are promising for potential new applications. Transparent glass–ceramics generally have two distinctive properties; they are nanocrystalline, and they have greater thermal stability than their parent glasses, frequently having an upper service temperatures of  $>800^\circ\text{C}$ .<sup>1–5</sup>

The advantage of transparent and translucent glass–ceramics over polycrystalline light-transmitting substances formed by conventional ceramic processes lies in the capacity and diversity of glass-forming processes. It is also easier to achieve transparency in a polycrystalline material by controlling nucleation and growth of small crystals in glass rather than by any other ceramic process.

Glass–ceramics materials may transmit visible light if either of the following condition are operative: (i) the crystallites are much smaller than the wavelength of visible light, or (ii) the

optical anisotropy within the crystals and refractive index difference between crystals and glass are very small.<sup>1–5</sup>

The aim of the present work was to prepare transparent mica glass–ceramic and to study the effect of addition of LiF and NaF on the crystallization behavior and transparency of the prepared glass–ceramic.

## 2. Experimental procedure

The chemical composition of base glass (K) is 37.96  $\text{SiO}_2$ –15.36  $\text{Al}_2\text{O}_3$ –6.32  $\text{B}_2\text{O}_3$ –18.1  $\text{MgO}$ –7.56  $\text{K}_2\text{O}$ –9F–5.6  $\text{TiO}_2$  (wt%). Standard reagent graded  $\text{SiO}_2$ ,  $\text{Al}_2\text{O}_3$ ,  $\text{MgCO}_3$ ,  $\text{MgF}_2$ ,  $\text{K}_2\text{CO}_3$ ,  $\text{TiO}_2$ ,  $\text{H}_3\text{BO}_3$ , NaF and LiF were used in the preparation of the glasses. Homogeneous mixtures of batches ( $\sim 100$  g), obtained by ball milling, were melted in alumina crucibles at  $1450^\circ\text{C}$  in an electric kiln for 2 h. The resulting melt was quenched in reheated steel mould and immediately annealed at  $500^\circ\text{C}$  to eliminate stress. A portion of the frit was hand milled in an agate mortar to obtain the glass powder for the thermal analysis. Crystallization kinetic of the glass powder was studied by differential scanning calorimeter (DSC-DSC-1500 Rheometric scientific USA calorimeter) with different heating rates (10, 15, 20  $^\circ\text{C}/\text{min}$ ). The crystallized phases of reheated samples were analyzed by X-ray diffraction (XRD) (Philips pw 1800

\* Corresponding author. Fax: +98 21 66005717.

E-mail addresses: [gh\\_mavad@yahoo.com](mailto:gh_mavad@yahoo.com), [ghasemzadeh@kiau.ac.ir](mailto:ghasemzadeh@kiau.ac.ir) (M. Ghasemzadeh).

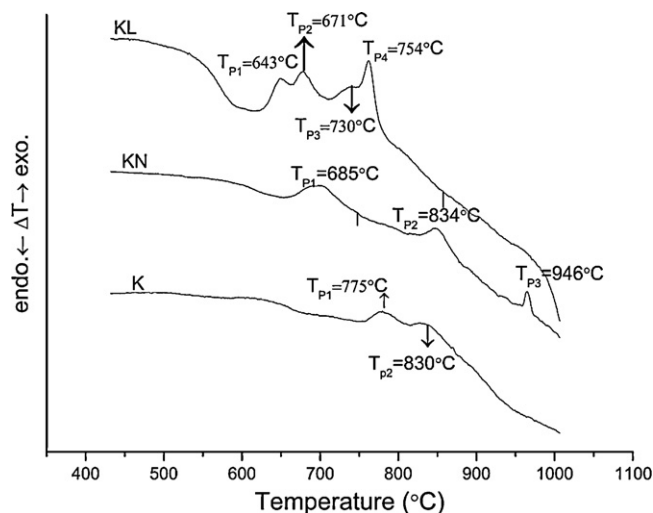


Fig. 1. DTA patterns of glass samples.

X-ray diffractometer). After immersing in 10 wt% HF solution for 7–20 s, microstructures of reheated samples were analyzed by SEM using Philips XL series (XL30) electron microscope. Crystallized bulk samples were ground and polished.

Optical transmission in UV–vis region was analyzed using a Cary 500 spectrophotometer using samples of thickness range (1 mm).

### 3. Theoretical basis

Eq. (1) has been used for crystallization evaluation, according to Kissinger's formula,<sup>6</sup> which has been used to calculate the activation energy of crystallization " $E_{CK}$ ".

$$\ln \left( \frac{\alpha}{T_p^2} \right) = \frac{-E_{CK}}{RT_p} + \text{constant} \quad (1)$$

By plotting the  $\ln(\alpha/T_p^2)$  vs.  $1/T_p$  a straight line should be obtained, from which the slope can be applied to determine  $E_{CK}$ . Matusia and Sakka<sup>7</sup> stated that Kissinger method is valid only when crystal growth occurs on a fixed number of nuclei. Incorrect values for the activation energy are obtained if a majority of the nuclei are formed during the DTA measurement, due to the number of nuclei continuously varying with  $\alpha$ . They have proposed a modified form of the Kissinger equation as given below:

$$\ln \left( \frac{\alpha^n}{T_p^2} \right) = \frac{-mE_C}{RT_p} + \text{constant} \quad (2)$$

where  $E_C$  is the correct or modified activation energy for crystallization and  $m$  is the dimension of growth, which can take

Table 1  
Properties of glass samples.

Sample	$T_g$ (°C)	$T_{P1}$ (°C)	$T = T_{P1} - T_g$	$E_C$ (kJ/mol)	$E_{CK}$ (kJ/mol)
K	634	775	141	405/72	235/2
KN	600	685	85	248	263
KL	540	643	103	624	583

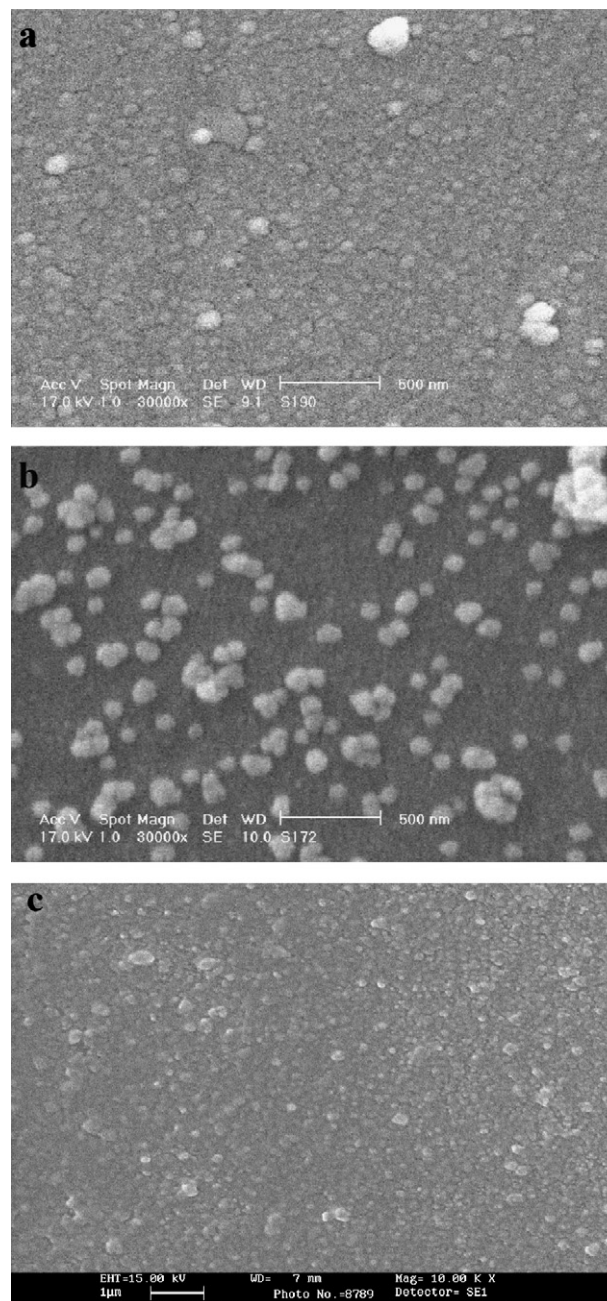


Fig. 2. SEM photographs of polished and chemically etched surfaces of parent glasses: (a) K, (b) KN and (c) KL.

values ranging from 1 to 3 ( $m=1, 2$  and  $3$ ) for one-, two- and three-dimensional growth, respectively.  $m=n-1$  when nucleation occurs during DTA and the number of nuclei in the glass is inversely proportional to  $\alpha$ . In addition, when surface crystallization predominates,  $m=n=1$  and Eq. (2) essentially reduces to the Kissinger equation. In other words,  $E_{CK}$  equals to  $E_C$ .

The Avrami exponent  $n$  can be evaluated by the modified Ozawa<sup>8</sup> equation using a multiple scan analysis technique: first volume fraction, " $x$ " is calculated at the same temperature from a number of crystallization exotherm under different heating rates by the ratio of partial area to the total area crystallization exotherm. After plotting  $\ln[-\ln(1-x)]$  vs.  $\ln \alpha$ , and if the data

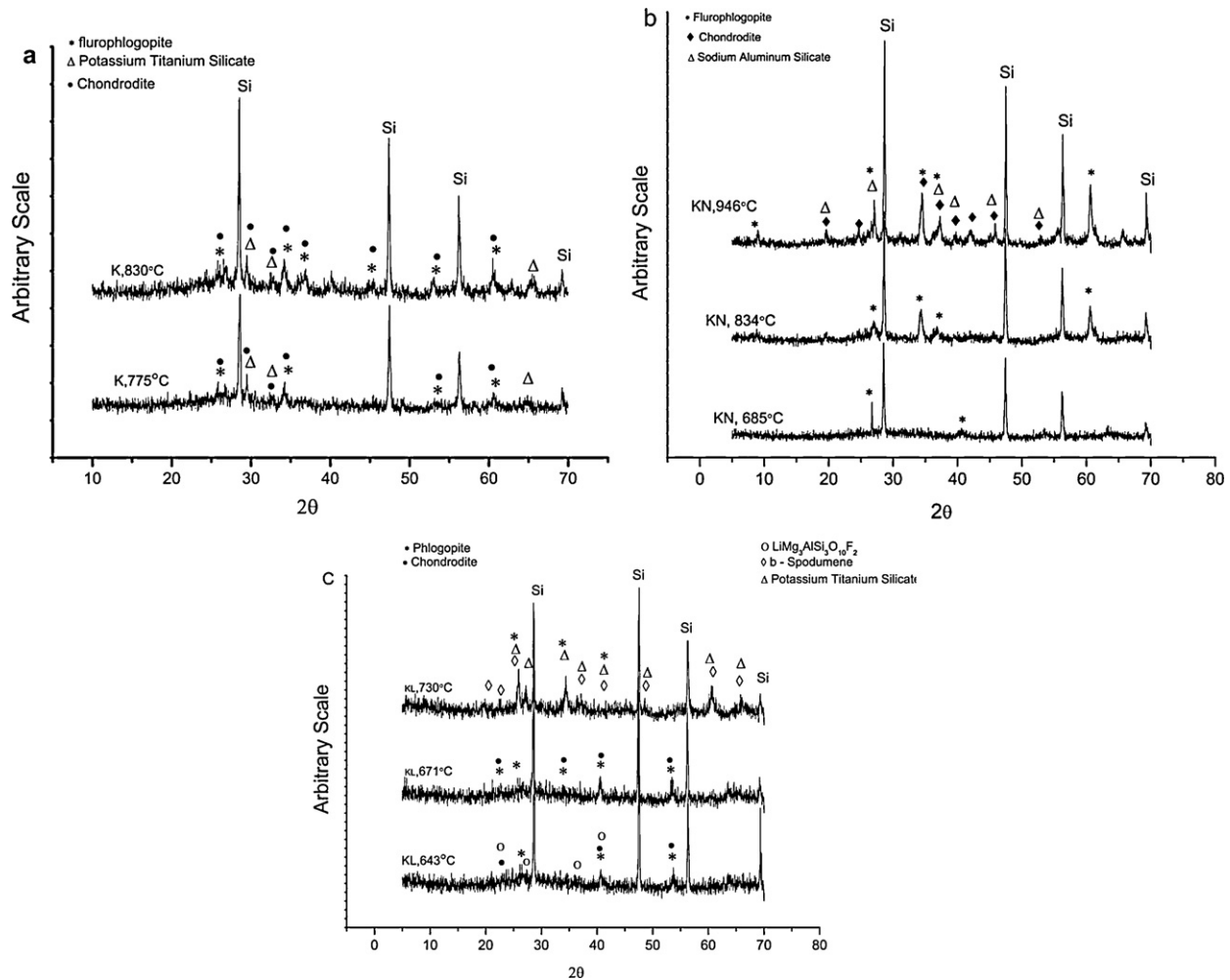


Fig. 3. XRD patterns of (a) K, (b) KN and (c) KL.

can be fitted to the linear function, then the slope of the function would be  $-n$ , i.e.:

$$\frac{d \ln[-\ln(1-x)]}{d \ln \alpha} = -n \quad (3)$$

#### 4. Results and discussion

Fig. 1 shows DTA curves of glass samples at the heating rate of  $10^\circ\text{C}/\text{min}$ . The glass transition temperature ( $T_g$ ), crystallization temperature ( $T_p$ ) and the thermal stability index  $\Delta T = T_p - T_g$  are listed in Table 1. The bigger the thermal stability index “ $\Delta T$ ”, indicates the more stable for glass and less tendency of crystallization. Note that  $T_{p1} \dots T_{p4}$  indicates the crystallization temperature of the phases in the system.

As it is clear from Table 1, the addition of 6 wt% LiF (KL) causes  $94^\circ\text{C}$  decrease on  $T_g$  of base glass (K) and  $132^\circ\text{C}$  decrease on  $T_p$ . Consequently, the thermal stability index  $\Delta T$  decreases by  $38^\circ\text{C}$  indicating an improvement on the crystallization of the glass. The addition of 6 wt% NaF (KN) causes a  $34^\circ\text{C}$  decrease in  $T_g$  and causes a  $90^\circ\text{C}$  in crystallization temperature. The thermal stability index decreases by  $56^\circ\text{C}$ .

Compared with  $\text{K}^+$ ,  $\text{Na}^+$  and  $\text{Li}^+$  have higher cationic field strength then the addition of NaF and LiF trend to phase separation, improving the nucleation and crystallization of glass. It is generally<sup>9</sup> accepted that fluorides, are immiscible in silicate melts leading to glass in glass phase separation by which numerous droplets of one glass are formed and dispersed in another one. The microstructure of the investigated annealed glasses clearly featured liquid–liquid phase separation, as shown in Fig. 2. The microstructures of KN and KL comprise numerous small droplets homogeneously distributed in glass matrix. Addition of NaF and LiF caused more intense phase separation in the system.

The values of  $E$  estimated by Kissinger and Matusita–Sakka methods are different, but the tendency is similar (Table 1). The values of  $n$  are found to be 0.57 and 1.8 for the first peak in KN and KL respectively. These values indicate that surface and bulk crystallizations in KN and KL respectively. The  $m$  value for the KL should be equal to  $n - 1$ . For the KN  $n = m = 0.57$  and the primary crystallization started from the surface of the sample.

Our understanding is that the base glass has fewer tendencies for phase separation than samples containing NaF and LiF. As mentioned in the literature, in comparison with base glass, the samples containing with  $\text{K}^+$ ,  $\text{Na}^+$  and  $\text{Li}^+$  have higher

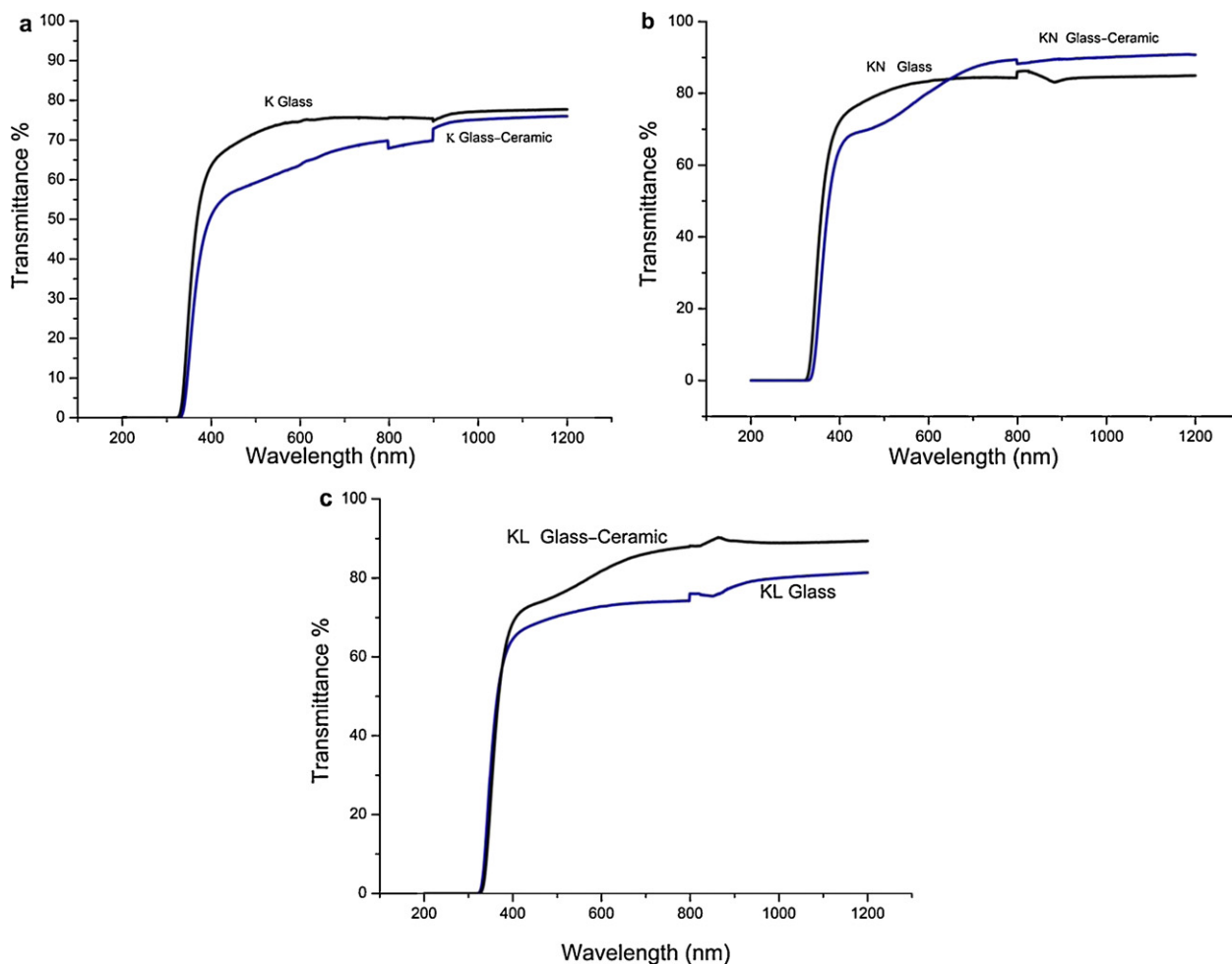


Fig. 4. UV-vis transmission curves of: (a) K samples (thickness of 1 mm), (b) KN samples (thickness of 1 mm) and (c) KL samples (thickness of 1 mm).

cationic field strength. That is why it seems reasonable to assume that the addition of NaF and LiF tend to more phase separation. It is generally accepted<sup>9</sup> that fluorides are immiscible in silicate melts leading to glass in glass phase separation by which numerous droplets of one glass are formed and dispersed in another one. The microstructure of the investigated annealed glasses featured liquid-liquid phase separation in small scale, as shown in Fig. 2a, which is much clear in higher magnification (Fig. 2b).

Besides, the addition of NaF and LiF has caused more intense phase separation in the system, as shown in Fig. 2(b) and (c).

Fig. 3 shows the XRD patterns of the glass-ceramics heat-treated at the crystallization peak temperatures. Major phases of sample K are fluorophlogopite and potassium titanium silicate and chondrodite. Except fluorophlogopite, chondrodite and sodium aluminum silicate are observed in glass-ceramic KN. With increasing the temperature, the relative intensity of phases has been increased. The XRD pattern of KL sample shows crystallization of fluorophlogopite, lithium magnesium aluminum fluoride silicate and chondrodite phases in the sample heat treated at 643 °C. In the KL sample heat treated in 671 °C for 2 h, fluorophlogopite and, chondrodite phases were crystallized, whereas in the case of KL sample heat-treated in 730 °C

fluorophlogopite,  $\beta$ -spodumene potassium titanium silicate phases were crystallized.

Optical transmission properties were measured for glasses and glass-ceramics K, KN and KL of 1 mm thickness. The results indicated that a microstructure with smaller grain size shows better transparency. The effect of temperature on transparency was vice versa.

Compared with the K glass (Fig. 4a), the transmission curved of the heat-treated glass-ceramic of K was all slightly shifted toward longer wavelengths. The spectrum shows that both glass and corresponding glass-ceramics of K have a transmission cutoff in the UV region at 330 nm. Fifty percent transmission occurs at approximately 364 nm >75% transmission occurs for wavelengths longer than approximately 600 nm. Like glass, glass-ceramics exhibit transparency in the visible region. Their cutoffs at 330 nm remained unchanged from that of the original glass. 50% transmission occurs at approximately 400 nm and >75% transmission occurs for wavelengths longer than approximately 980 nm. The addition of NaF in KN is observed to have effect on the transparency of the heat-treated glass sample. From Fig. 4b, 50% transmission at approximately 362 nm and >75% transmission occurs for wavelengths longer than approximately 420 nm. In the form of glass-ceramics 50% transmission



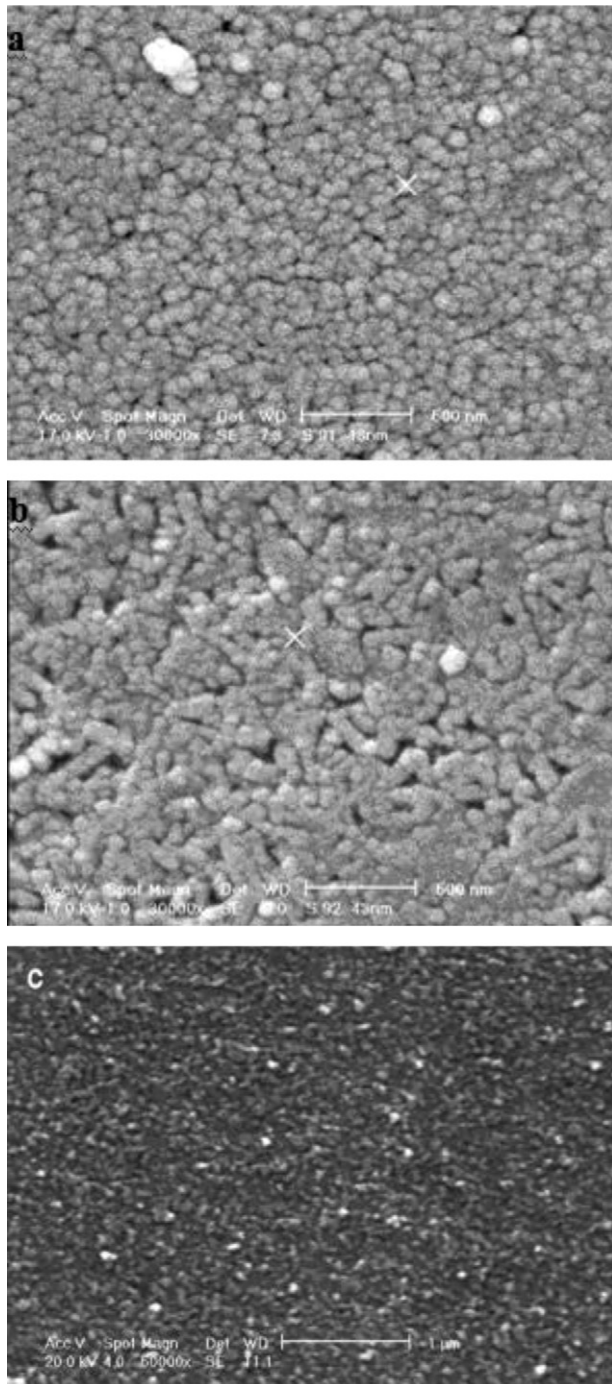


Fig. 5. Microstructure of (a) KN after heat treatment at 685 °C for 2 h; (b) KN after heat treatment at 946 °C for 2 h and (c) KL after heat treatment at 643 °C for 2 h.

occurs at approximately 376 nm and >75% transmission occurs for wavelengths longer than approximately 543 nm. In the glass of KL, 50% transmission occurs at approximately 366 nm and >75% transmission occurs for wavelengths longer than approximately 798 nm. In the form of glass–ceramics 50% transmission occurs at approximately 369 nm and >75% transmission occurs for wavelengths longer than approximately 488 nm (Fig. 4c).

Fig. 5 shows the microstructure of KN that heat-treated at the crystallization peak temperatures. SEM of optically transparent

KN sample heat-treated for 2 h at 685 °C shows the quasi-spherical grains with nano size were precipitated uniformly (Fig. 5a). The size of crystal grain increased with increasing temperature after being heat-treated for 2 h at 946 °C (Fig. 5b). SEM of optically transparent KL sample heat-treated for 2 h at 643 °C shows the quasi-spherical grains with nano size were precipitated uniformly (Fig. 5c). A glass–ceramic will lose its transparency when the crystallization process is carried out because of the difference in the refractive index between raw glass and precipitated crystals.<sup>1</sup> The glass–ceramic can remain transparent if fine grains are precipitated, but will turn opaque when large grain appear, due to the large grain-size effect on opacity.

Base sample does not transmit any light below 330 nm. When it was heat treated at 775 °C [become a glass–ceramic], the edge of light transmission switch to higher wave length. In this samples, 50% of the light was passed through the sample at 364 nm and 75% at near the 600 nm.

Addition of LiF and NaF affects the light transmission. The sample L<sub>0</sub>LiF<sub>6</sub> does not transmit any light in less than 306 nm. If they were heat treated at 671 °C (in the case of LiF) and 685 °C (in the case of NaF), the transmission of the light was altered and switched to higher wave length and transparency was reduced.

## 5. Conclusion

Controlled crystallization of glasses in the system of MgO–SiO<sub>2</sub>–Al<sub>2</sub>O<sub>3</sub>–K<sub>2</sub>O–B<sub>2</sub>O<sub>3</sub>–F, produced transparent mica glass–ceramics. It is believed that phase separation in glass is one of the most important factor for the high nucleation rate and consequently for the relatively small grain growth, resulting in the formation of transparent glass–ceramics. The results indicated that liquid–liquid phase separation exists in small scale. After heat treatment, the separation of mica phase was occurred.

The transmission observed in the basic composition (K), is related to the microstructural features of the sample K. It seems to us that low transmission (less than 80% at 600 nm) may be due to this feature.

Heat-treatment at the crystallization peak temperatures changed the optical characteristics of the KN samples. The size of crystal grain increased with increasing temperature after heat-treated for 2 h at 946 °C. SEM of optically transparent KL sample heat-treated for 2 h at 643 °C showed quasi-spherical grains with nano size.

Besides, the addition of NaF and LiF has caused more intense phase separation in the system.

## References

1. Abdel-Hameed SAM, Ghoniem NA, Saad EA, Margha FH. Effect of fluoride ions on the preparation of transparent glass ceramics based on crystallization of barium borates. *Ceram Int* 2005;**31**:499–505.
2. Stryjak AJ, Mcmillan PW. Microstructure and properties of transparent glass–ceramics. *J Mater Sci* 1978;**13**:1794–804.
3. Taruta S, Suzuki M. Preparation and ionic conductivity of transparent glass–ceramics containing a large quantity of lithium–mica. *J Non-Cryst Solids* 2008;**354**:848–55.

4. Taruta S, Sakata M, Yamaguch T, Kitajima K. Crystallization process and some properties of novel transparent machinable calcium–mica glass–ceramics. *Ceram Int* 2008;**38**:75–9.
5. Trauta S, Ichinose T, Yamaguch T, Kitajima K. Preparation of transparent lithium–mica glass–ceramics. *J Non-Cryst Solids* 2006;**352**:5556–63.
6. Kissinger HE. Reaction kinetic in differential thermal analysis. *Anal Chem* 1957;**29**:1702–6.
7. Matusita K, Sakka S. Kinetic Study on crystallization of glass by differential thermal analysis-criterion on application of Kissinger plot. *J Non-Cryst Solids* 1980;**38&39**:741.
8. Ozawa T. Kinetics of non-isothermal crystallization. *Polymer* 1971;**12**:150–8.
9. Radonjic L, Nikolic L. The effect of fluorine source and concentration on the crystallization of machinable glass–ceramics. *J Eur Ceram Soc* 1991;**7**: 11–6.